Submillimetre images of dusty debris around nearby stars

Wayne S. Holland*, Jane S. Greaves*, B. Zuckerman†, R. A. Webb†, Chris McCarthy†, Iain M. Coulson*, D. M. Walther‡, William R. F. Dent§, Walter K. Gear‖ & Ian Robson*

* *Joint Astronomy Centre, 660 N. A'ohōkū Place, Hilo, Hawaii 96720, USA*
† *Department of Physics & Astronomy, University of California, Los Angeles, Los Angeles, California 90095, USA*
‡ *Gemini 8m Telescopes Project, 180 N. Kinoole Street No. 207, Hilo, Hawaii 96720, USA*
§ *Royal Observatory, Blackford Hill, Edinburgh EH9 3HJ, UK*
‖ *Mullard Space Science Laboratory, Holmbury St Mary, Dorking, Surrey RH5 6NT, UK*

....

Indirect detections of massive—presumably Jupiter-like—planets orbiting nearby Sun-like stars have recently been reported[1,2]. Rocky, Earth-like planets are much more difficult to detect, but clues to their possible existence can nevertheless be obtained from observations of the circumstellar debris disks of dust from which they form. The presence of such disks has been inferred[3] from excess far-infrared emission but, with the exception of β Pictoris[4], it has proved difficult to image these structures directly as starlight dominates the faint light scattered by the dust[5]. A more promising approach is to attempt to image the thermal emission from the dust grains at submillimetre wavelengths[6,7]. Here we present images of such emission around Fomalhaut, β Pictoris and Vega. For each star, dust emission is detected from regions comparable in size to the Sun's Kuiper belt of comets. The total dust mass surrounding each star is only a few lunar masses, so any Earth-like planets present must already have formed. The presence of the central cavity, approximately the size of Neptune's orbit, that we detect in the emission from Fomalhaut may indeed be the signature of such planets.

The observations were made during the period April–October 1997, using the Submillimetre Common-User Bolometer Array (SCUBA)[8] at the James Clerk Maxwell Telescope (JCMT) on Mauna Kea, Hawaii. Although data were taken at wavelengths of 450 and 850 μm simultaneously, only the 850-μm data are discussed here, as observing conditions were poor for good-quality 450-μm work. The full-width at half-maximum (FWHM) beam size at 850 μm was 14 arcsec, and the array field of view has a diameter of 2.3 arcmin. Telescope pointing was checked before and after each observation on a nearby quasar, with r.m.s. pointing errors of <2 arcsec. The data were analysed using the SCUBA User Reduction Facility[9]. Table 1 details the integration times and flux measurements, and the final maps are presented in Fig. 1. The fluxes quoted in Table 1 are from the raw maps, whilst the images shown in Fig. 1 have been smoothed slightly by a 7-arcsec gaussian (FWHM) to improve the signal-to-noise ratio.

The 850-μm image of Fomalhaut (Fig. 1a) shows that the dust emission peaks at two positions offset from the star by ~10 arcsec to the north and the south. This image is consistent with an edge-on torus ('doughnut') structure with a central cavity with much less dust emission. At the outer edge it is not possible to distinguish between an abrupt drop or a moderate density decline with radius. It was anticipated that the dusty disk would be seen nearly edge-on because Fomalhaut's projected rotation velocity of 100 km s^{-1} (ref. 10) is consistent with a spin axis nearly in the plane of the sky. After deconvolution from the 14-arcsec beam (at the map half-power points), the major axis is 41 ± 2 arcsec, or 315 ± 15 astronomical units (AU; where 1 AU is the mean Sun–Earth distance) at a position angle (PA) of 162 ± 4°. The minor axis is ~18 ± 2 arcsec deconvolved, and hence implies a torus inclination angle of 64 ± 5° (an inclination angle of 0° indicates a spin axis pointing along our line of sight). These dimensions compare favourably with previous estimates[11] at 100 μm. The data also agree well with the low signal-to-noise point-by-point map and flux estimates of an earlier study at the JCMT[6].

The regions of peak dust emission are ~80 AU from the star. This is comparable to the distance of the Kuiper belt of comets in our own Solar System which begins just beyond the orbit of Pluto[12]. However, the dust grains are warmer than in the Kuiper belt because Fomalhaut is ~16 times more luminous than the Sun. At a distance of 80 AU from Fomalhaut, particles sufficiently large (diameter ~60 μm) to radiate like black-bodies at wavelengths of 60–100 μm will be at ~70 K. (In the Solar System this value is measured at Uranus' distance from the Sun.) This is the temperature that characterizes the far-infrared emission from Fomalhaut[10], so the far-infrared and submillimetre data are consistent with a grain population that is well mixed in space. A variety of grain sizes is needed within this population to explain the spectral energy distribution[6].

The central cavity is ~8 arcsec (60 AU) in diameter, approximately the size of Neptune's orbit. This observed size agrees reasonably well with the size of the inner cavity deduced from models of the far-infrared emission[13]. One plausible explanation is that this region has been cleared of gas and dust by the formation of planetesimals. However, other mechanisms could produce a central cavity; for example, sublimation of ice-mantle grains[14], or radiation-grain drag (Poynting–Robertson effect)[6]. We also note that as cratering records in the inner Solar System indicate debris clearing times significantly longer than the estimated age of Fomalhaut (200 Myr; ref. 15), planets may exist even within the dusty region. If so, their gravity could extend the vertical distribution of particles, enabling the dust to absorb more stellar light and thus enhancing the far-infrared emission[16].

β Pic is one of the youngest stars in the solar vicinity at an age of ~10–100 Myr (ref. 17). The 850-μm map (Fig. 1b) shows a clear

Table 1 Source and observation summary

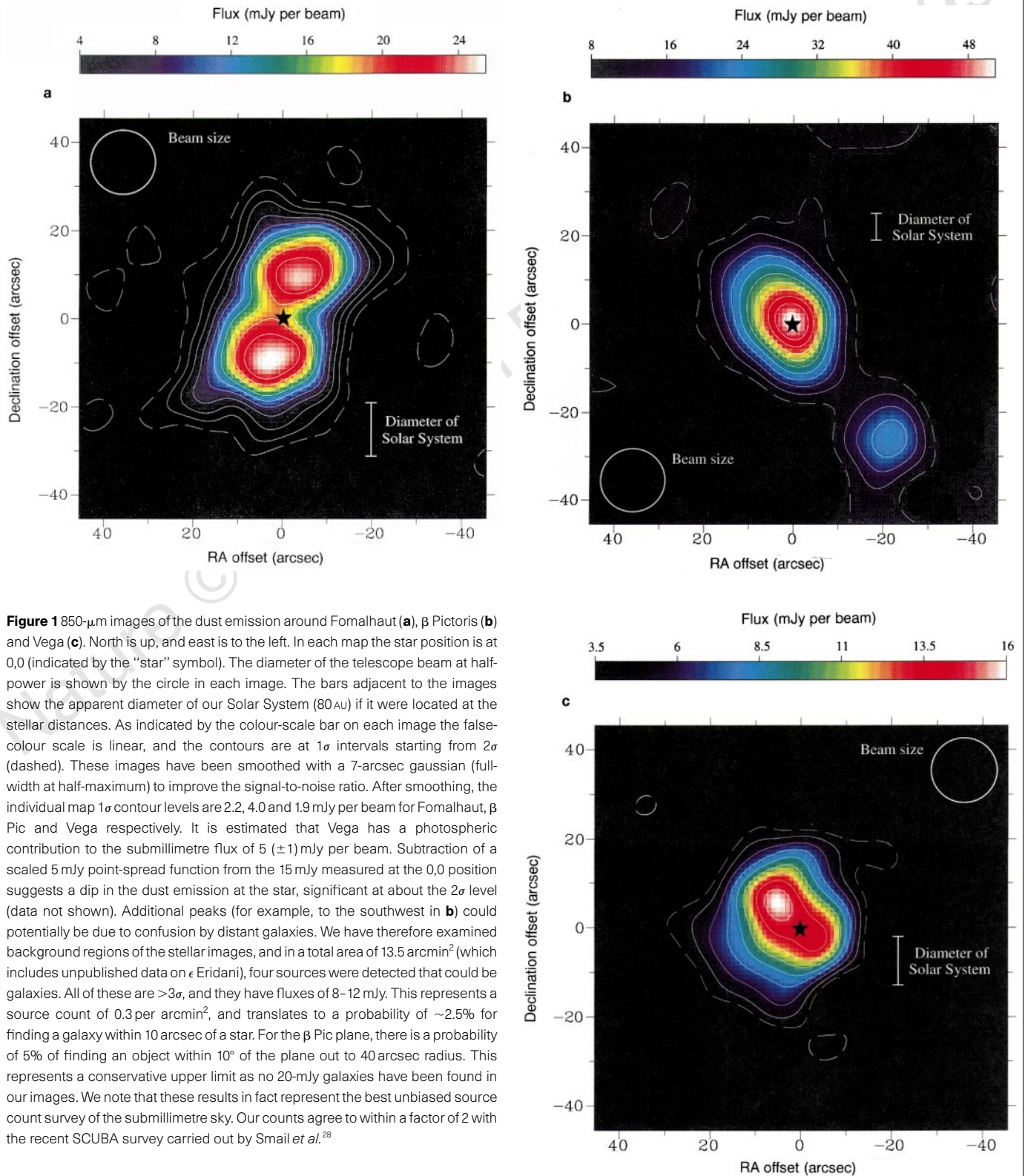| Star	RA dec. (J2000)	Type	Distance* (pc)	Integration time (h)	Dust peak† δRA (arcsec)	δdec. (arcsec)	850-μm flux (mJy per beam)	Dust mass‡ (M_{moon})
α Piscis Austrinus (Fomalhaut)	22 h 57 min 39.0 s −29° 37′ 20.0″	A3V	7.69	5.0	3.5W 3.0E	9.7N 9.0S	28.9 ± 3.7 28.0 ± 3.7	
					Integrated§:		81.0 ± 7.2	1.5
β Pictoris	05 h 47 min 17.1 s −51° 04′ 00.0″	A5V	19.3	5.3	0.8N 21.4W	9.7N 25.9S	58.3 ± 6.5 19.1 ± 6.5	
					Integrated§:		104.3 ± 10.0	7.8
α Lyrae (Vega)	18 h 36 min 56.3 s +38° 47′ 01.2″	A0V	7.76	8.6	5.9E	7.1N	17.3 ± 3.0	
					Integrated§:		45.7 ± 5.4	0.7

* Distances are from the Hipparcos catalogue (ESA SP-1200, 1997).
† Estimated errors in the dust peak centroid positions are ±1 arcsec.
‡ Estimated dust masses are given in lunar masses ($M_{moon} = 7 \times 10^{25}$ kg).
§ Integrated fluxes (mJy) are measured within a radius of 30 arcsec (40 arcsec for β Pictoris) from the star.

elongation of the dust emission with a PA of $32 \pm 4°$, which, given the resolution of the JCMT beam, is consistent with optical and near-infrared images (for example, $30.7 \pm 0.7°$; ref. 18). The dust emission peaks on the stellar position and extends along the major axis to an observed radius of ~13 arcsec (250 AU). The deconvolved size of the disk is $22 \times 11 (\pm 3)$ arcsec (that is, unresolved in the minor axis), giving an inclination angle of $>60°$.

In addition to the main disk, separated patches of emission are seen further out in Fig. 1b, two of which are fairly closely aligned with the plane of the disk. The most prominent of these (RA 21 W, dec 26 S) lies at a PA of 37 (±6)° and has a flux of 19.1 mJy per beam. This is almost certainly a real detection and has a PA consistent with a feature in the disk plane. This could be a fragmented outer part of the disk (although such a feature does not appear in optical images),

Figure 1 850-μm images of the dust emission around Fomalhaut (**a**), β Pictoris (**b**) and Vega (**c**). North is up, and east is to the left. In each map the star position is at 0,0 (indicated by the "star" symbol). The diameter of the telescope beam at half-power is shown by the circle in each image. The bars adjacent to the images show the apparent diameter of our Solar System (80 AU) if it were located at the stellar distances. As indicated by the colour-scale bar on each image the false-colour scale is linear, and the contours are at 1σ intervals starting from 2σ (dashed). These images have been smoothed with a 7-arcsec gaussian (full-width at half-maximum) to improve the signal-to-noise ratio. After smoothing, the individual map 1σ contour levels are 2.2, 4.0 and 1.9 mJy per beam for Fomalhaut, β Pic and Vega respectively. It is estimated that Vega has a photospheric contribution to the submillimetre flux of 5 (±1) mJy per beam. Subtraction of a scaled 5 mJy point-spread function from the 15 mJy measured at the 0,0 position suggests a dip in the dust emission at the star, significant at about the 2σ level (data not shown). Additional peaks (for example, to the southwest in **b**) could potentially be due to confusion by distant galaxies. We have therefore examined background regions of the stellar images, and in a total area of 13.5 arcmin² (which includes unpublished data on ε Eridani), four sources were detected that could be galaxies. All of these are $>3\sigma$, and they have fluxes of 8–12 mJy. This represents a source count of 0.3 per arcmin², and translates to a probability of ~2.5% for finding a galaxy within 10 arcsec of a star. For the β Pic plane, there is a probability of 5% of finding an object within 10° of the plane out to 40 arcsec radius. This represents a conservative upper limit as no 20-mJy galaxies have been found in our images. We note that these results in fact represent the best unbiased source count survey of the submillimetre sky. Our counts agree to within a factor of 2 with the recent SCUBA survey carried out by Smail *et al.*[28]

or possibly a second disk about a low-mass companion (which would explain why there is no peak of corresponding brightness to the northeast). If the age of the companion is <10 Myr, then such a disk might not have dissipated, and could be primordial like those around T-Tauri stars, in contrast to the much older debris disks seen around Fomalhaut and Vega. However, recent deep R-band data at a wavelength of 680 nm revealed no companion to a limiting magnitude of ~22 (compare with an R-band magnitude ~4 for β Pic) within 6 arcsec of the southwest offset source (P. Kalas and B. A. Smith, personal communications). On the basis of the cooling models of Burrows et al.[24], and an assumed age of 30 Myr for β Pic, the mass of any companion at the offset source position is less than 10 Jupiter masses. Finally, we cannot rule out a coincidental alignment with a background object, such as a distant galaxy, and this possibility is further discussed in the legend to Fig. 1.

The 850-μm map of Vega (Fig. 1c) shows an extended, approximately circular structure with dimensions $24 \times 21 (\pm 3)$ arcsec (deconvolved from the beam size), somewhat smaller than the $35(\pm 5)$ arcsec derived from far-infrared measurements[19]. Within this is an elongated bright central region orientated northeast–southwest. The peak is 9 arcsec (70 AU) to the northeast of the star's position, and this is unlikely to be an artefact, as it is consistent with the low signal-to-noise detection in the earlier JCMT study[6]. This region has a superficial resemblance to the Fomalhaut image. However, interpreting this as a torus or edge-on disk encounters two serious problems. The low projected rotational velocity (22 km s^{-1}) and a spectral line analysis[20] suggest that the star is rapidly rotating and viewed close to pole-on. Also, the extended dust emission is roughly circular, favouring a pole-on geometry.

The northeast peak is brighter than the corresponding emission southwest of the star by ~2σ, and so it is unclear whether these are separate objects or part of a symmetrical structure. A symmetrical elongation could be due to perturbation of a disk by a planet, as hypothesized for the warped disk of β Pic[21]. Alternatively, a single peak could be interpreted as an object in orbit about Vega,

surrounded by a concentration of dust. However, circumplanetary disks (such as the one from which Jupiter's moons formed) are expected to dissipate much more rapidly than circumstellar disks, making the presence of such a structure unlikely at Vega's age of 350 Myr (ref. 22). Alternatively, if rocky planetary bodies have formed, the collision of two such objects could inject new dust into the disk, but the objects involved would have to be exceedingly large 'planetesimals' to shed a substantial fraction of a lunar mass in dust. Additional observations were made to investigate this offset peak: first, it was detected by SCUBA at 1,350 μm with single point photometry. The 850- and 1,350-μm fluxes imply a spectral index of 2.7, consistent with previous observations of dust around young stars[23]. Second, a coronographic image of Vega at 2.2 μm, using the Near-Infrared Camera on the Keck 10-m telescope, revealed no companion down to a limiting magnitude of 16. This rules out orbiting companions with masses greater than 12 Jupiter masses, based on models of 350-Myr-old 'superplanets'[24].

We have compared the amounts of dust observed both to the Solar System and to other stars with younger ages. The ages of Fomalhaut, β Pic and Vega—tens to hundreds of millions of years—span a range of particular interest in the history of our Solar System. The formation of giant planets probably occurred within ~10 Myr, and the Earth within 100 Myr. In addition, the period of heavy bombardment in the inner Solar System by cometary and asteroidal-sized objects lasted ~600 Myr (ref. 25).

Dust masses were estimated (Table 1) from the 850-μm integrated fluxes using grain temperatures deduced from far-infrared data[10]. As the composition and size of the circumstellar grains remain uncertain, we adopt an 850-μm mass absorption coefficient for dust (K_{abs}) of 1.7 cm^2 g^{-1} for consistency and ease of comparison with the previous best measured dust masses[6] (the range of values of K_{abs} is further discussed in ref. 26). There may be an associated gas component, but, for example, a sensitive search for atomic hydrogen around β Pic has shown that the gas-to-dust ratio is at least 10 times lower than in the interstellar medium, suggesting most of the gas has been dispersed[27]. The derived dust masses are of the order of the Moon's mass, and agree well with the previous values[6]. These masses are plotted in Fig. 2 as a function of stellar age. The apparent decrease in the mass of dust particles with time can be attributed to accumulation into planets, or dispersal by mechanisms such as the Poynting–Robertson effect, stellar winds, and sublimation. Whichever of these mechanisms dominates, the dust masses appear to decrease rapidly between ages of 1 and 100 Myr. Figure 2 suggests that circumstellar dust falls below an Earth mass (80 Moon masses) at an estimated age of 10 Myr. Thus at the ages of Fomalhaut, β Pic and Vega, planetesimal accumulation must be well underway if planetary systems are to form.

Our submillimetre images have provided the first detailed information on the morphology of the dust emission around nearby stars. Ice sublimation and Poynting–Robertson drag need to be investigated as possible causes of the central cavity at Fomalhaut, before planet formation becomes the adopted model. If the offset peaks for Vega and β Pic are physically associated with these stars, then compelling models need to be devised. We plan further submillimetre imaging at 450 μm, with 8-arcsec resolution. Such data may reveal details such as warping, a possible signature of planetary perturbations, and, when combined with longer-wavelength results, should enable investigations of grain growth processes. □
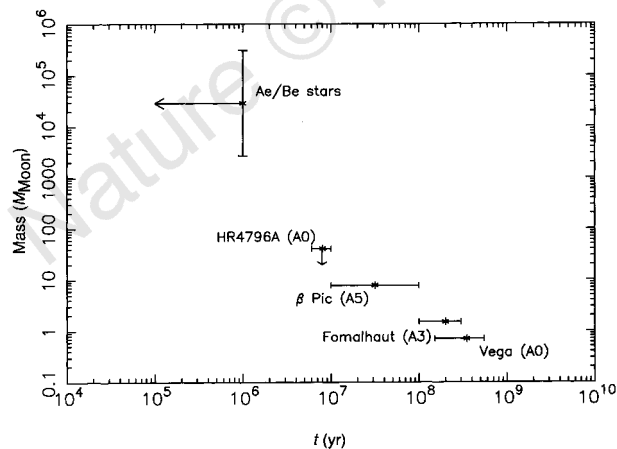

Figure 2 Circumstellar dust masses plotted as a function of stellar age (t). The data for Fomalhaut, β Pic and Vega (stellar types A0 to A5) are compared to JCMT observations of younger high-mass stars. These include an upper limit for HR4796A[29] and detections of a sample of emission-line A and B type stars[30]. These stars have ages of only 0.1-1 Myr, and are often still associated with their parental molecular clouds. Horizontal error bars indicate the uncertainties in the stellar ages, and for the Ae/Be stars, the vertical error bar is the range of masses around several stars. Mass uncertainties depend on the assumed grain temperatures and absorption coefficients. The plotted values could be up to a factor of 2 lower (if all the grains are at the highest dust temperatures measured in the far-infrared[10]), and upper limits are essentially unconstrained, as very large grains could contribute substantial mass, while adding little to the total emitting area at submillimetre wavelengths.

1. Mayor, M. & Queloz, D. A. Jupiter-sized companion to a solar-type star. *Nature* **378,** 355–359 (1995).
2. Butler, P. & Marcy, G. Detection of extrasolar planets. *Annu. Rev. Astron. Astrophys.* (in the press).
3. Aumann, H. H. *et al.* Discovery of a shell around α Lyrae. *Astrophys. J.* **278,** L23–L27 (1984).
4. Smith, B. A. & Terrile, R. J. The circumstellar disk around β Pictoris. *Science* **226,** 1421–1424 (1984).
5. Kalas, P. & Jewitt, D. The detectability of β Pic-like circumstellar disks around nearby main-sequence stars. *Astron. J.* **111,** 1347–1355 (1996).
6. Zuckerman, B. & Becklin, E. E. Submillimetre studies of main-sequence stars. *Astrophys. J.* **414,** 793–802 (1993).

7. Chini, R., Krügel, E., Kreysa, E., Shustov, B. & Tutukov, A. Dust disks around Vega-type stars. *Astron. Astrophys.* **252,** 220–228 (1991).
8. Holland, W. S. *et al.* in *Advanced Technology MMW, Radio and Terahertz Telescopes* (ed Phillips, T.) (*Proc. SPIE* 3357, in the press).
9. Jenness, T. & Lightfoot, J. F. in *Starlink User Manual* Vol. 216 (1997).
10. Backman, D. E. & Paresce, F. in *Protostars and Planets III* (eds Levy, E. H. & Lunine, J. I.) 1253–1304 (Univ. Arizona Press, Tucson, 1993).
11. Lester, D., Harvey, P., Smith, B., Colomé, C. & Low, F. The far-IR size of the dust cloud around Fomalhaut. *Bull. Am. Astron. Soc.* **21,** 1085–1086 (1989).
12. Backman, D. E., Dasgupta, A. & Stencel, R. E. Model of a Kuiper Belt small grain population and resulting far-IR emission. *Astrophys. J.* **450,** L35–L38 (1995).
13. Harvey, P. M., Smith, B. J., DiFrancesco, J., Colomé, C. & Low, F. J. Far-IR constraints on dust shells around Vega-like stars. *Astrophys. J.* **471,** 973–978 (1996).
14. Jura, M. *et al.* A proto-cometary cloud around HR 4796A? *Astrophys. J.* (submitted).
15. Barrado y Navascues, D., Stauffer, J. R., Hartmann, L. & Balachandran, S. C. The age of Gliese 879 and Fomalhaut. *Astrophys. J.* **475,** 313–321 (1997).
16. Nakano, T. Formation of planets around stars of various masses—II. Stars of two and three solar masses and the origin and evolution of interstellar dust clouds. *Mon. Not. R. Astron. Soc.* **230,** 551–571 (1988).
17. Armitage, P. J. & Pringle, J. E. Radiation-induced warping of protostellar accretion disks. *Astrophys. J.* **488,** L47–L50 (1997).
18. Kalas, P. & Jewitt, D. Asymmetries in the β Pictoris disk. *Astron. J.* **110,** 794–804 (1995).
19. van der Bliek, N. S., Prusti, T. & Waters, L. B. F. M. Vega: smaller dust grains in a larger shell. *Astron. Astrophys.* **285,** 229–232 (1994).
20. Gulliver, A. F., Hill, G. & Adelman, S. J. Vega: a rapidly rotating pole-on star. *Astrophys. J.* **429,** L81–L84 (1994).
21. Heap, S. R. *et al.* Hubble/STIS coronographic imagery of β Pictoris. *Bull. Am. Astron. Soc.* **29,** 1285 (1997).
22. Maeder, A. & Meynet, G. Tables of evolutionary star models from 0.85 to 120 solar masses, with overshooting and mass loss. *Astron. Astrophys. Suppl.* **76,** 411–425 (1988).
23. Mannings, V. G. & Emerson, J. P. Dust in disks around T-Tauri stars: Grain growth? *Mon. Not. R. Astron. Soc.* **267,** 361–378 (1994).
24. Burrows, A. *et al.* in *Brown Dwarfs and Extrasolar Planets* (eds Rebolo, R., Martin, E. L. & Zapatero-Osorio, M. R.) 354–369 (ASP conf. ser. Vol. 134, 1998).
25. Maher, K. A. & Stevenson, D. J. Impact frustration of the origin of life. *Nature* **331,** 612–614 (1988).
26. Pollack, J. B. *et al.* Composition and radiative properties of grains in molecular clouds and accretion disks. *Astrophys. J.* **421,** 615–639 (1994).
27. Freudling, W., Lagrange, A.-M., Vidal-Madjar, A., Ferlet, R. & Forveille, T. Gas around β Pictoris: an upper limit on the HI content. *Astron. Astrophys.* **301,** 231–235 (1995).
28. Smail, I., Ivison, R. J. & Blain, A. W. A deep submillimetre survey of lensing clusters: A new window on galaxy formation and evolution. *Astrophys. J.* **490,** L5–L8 (1997).
29. Jura, M. *et al.* The fate of the solid matter orbiting HR4796A. *Astrophys. J.* **445,** 45–53 (1995).
30. Mannings, V. G. Submillimetre observations of Herbig Ae/Be systems. *Mon. Not. R. Astron. Soc.* **271,** 587–600 (1994).

Shallow mixing in the solar photosphere inferred from revised beryllium abundances

Suchitra C. Balachandran & Roger A. Bell

Department of Astronomy, University of Maryland, College Park, Maryland 20742, USA

The chemical compositions of the Sun and meteorites are the benchmarks against which the abundances of elements in all other astronomical objects are compared. A long-standing problem[1] has been the abundance of lithium in the Sun's photosphere, which is ~140 times less than the meteoritic value (which represents the lithium abundance at the time the Solar System formed). This depletion requires that material from the photosphere be transported below the convective zone into regions where the temperature is high enough that nuclear processing can remove lithium. The models[2,3] best able to do so simultaneously deplete beryllium by about a factor of two, which is consistent with previous measurements[4,5] of the beryllium abundance in the solar photosphere. But here we show that these previous measurements are in error, because they did not fully account for the continuous opacity in the ultraviolet region of the spectrum where the beryllium lines are observed. We find that, after

correcting for this opacity, solar beryllium is not depleted at all with respect to the meteoritic value. This implies that mixing in the solar photosphere is more superficial than had hitherto been supposed, consistent with the shallow mixing inferred from recent helioseismic data[6].

The only lines available for ground-based Be measurements are the Be II resonance lines at 3,130.42 and 3,131.06 Å near the atmospheric ultraviolet (UV) cut-off. In addition to the analytical difficulty of obtaining accurate abundances from crowded spectral regions, a singular problem plagues UV measurements: the uncertain UV opacity. An increase in this opacity is demanded by theoretical models of the solar atmosphere which consistently overpredict the UV flux[7]. Although the suggestion has been made that this mismatch is due to the insufficient inclusion of line opacity[8], comparisons of high-resolution solar and synthetic spectra have shown that when all of the spectral features are reasonably well accounted for, the calculated solar flux remains too large[9]. Thus, the 'missing UV opacity' must be due to a continuous opacity or to a very large number of very weak lines[10] which essentially mimic a continuous opacity.

To quantify the 'missing UV opacity' in the solar models, we have taken the empirical approach of requiring the UV A–X electronic transitions of the OH molecule to yield the same oxygen abundance as the vibrational–rotational OH transitions in the infrared (IR). The IR transitions, regarded as one of the more reliable oxygen-abundance indicators[11], are used to obtain an accurate oxygen abundance in the Sun. The oscillator strengths of the UV lines are accurately known, with experimental and theoretical values agreeing to within 10% (ref. 12). If the continuous opacity in the Sun is not fully accounted for in the synthetic spectral calculations, the calculated UV OH features will be stronger than observed. The mismatch between the observed and predicted line strengths is attributable to the 'missing UV opacity'.

We used the high-resolution ($\lambda/\Delta\lambda = 348,000$) solar flux spectral atlas[13] for our investigation. We searched an 80-Å region of the solar spectrum from 3,100 to 3,180 Å for clean (unblended) OH features. Fourteen features satisfied our condition that the sole contribution to the synthetic line comes from the OH feature. The observed feature may, of course, contain blends not identified in our list of lines[9]. Our empirical process therefore produces a lower limit to the 'missing' opacity. Three model solar atmospheres were used in our analysis: the Holweger–Müller (HM) empirical model[14], the Kurucz solar model without overshoot[15] and the updated OSMARCS model[16]. As OH is a trace species in the solar atmosphere, the oxygen abundance derived from OH lines is sensitively dependent on the model characteristics. Using the solar equivalent widths for the IR vibrational–rotational OH lines[17], the following values were obtained for the oxygen abundance on a logarithmic scale where the abundance of hydrogen is 12: $\log\epsilon(O) = 8.91 \pm 0.02$ (HM), 8.80 ± 0.02 (Kurucz) and 8.75 ± 0.02 (OSMARCS). Synthetic spectra of UV OH lines generated from each model atmosphere and its corresponding IR-based oxygen abundance produced lines of identical strength, indicating that the UV and IR OH lines are formed in the same part of the atmosphere and under similar conditions. Our differential use of the OH lines as a benchmark for the oxygen abundance therefore precludes the need to know the absolute value of the oxygen abundance with high accuracy.

Synthetic UV spectra were calculated under the condition of local thermodynamic equilibrium. The following opacities were included in the calculation of the synthetic solar spectrum: H_{bf}, H_{bf}^-, H_{ff}^-, H_{2bf}^+, H_{2ff}^+, H and He Rayleigh scattering, He_{ff}^- and electron scattering; here subscript bf indicates bound–free, and ff indicates free–free. Metal bound–free opacities were not used in our calculation. Opacity Project (an international collaboration to calculate atomic data for stellar opacity computations) calculations of Si I and Mg I bound–free opacities[18] show that they are relatively small at optical depth $(\tau)(3,100) = 0.1$, being roughly 1% and 8.5% respectively of the